Community dynamics and ecosystem simplification in a high-CO_2 ocean

Kristy J. Kroeker[a,1], Maria Cristina Gambi[b], and Fiorenza Micheli[c]

[a]Bodega Marine Laboratory, University of California, Davis, Bodega Bay, CA 94923; [b]Functional and Evolutionary Ecology Laboratory, Stazione Zoologica Anton Dohrn, 80121 Naples, Italy; and [c]Hopkins Marine Station, Department of Biology, Stanford University, Pacific Grove, CA 93950

Edited by David M. Karl, University of Hawaii, Honolulu, HI, and approved June 7, 2013 (received for review September 20, 2012)

Disturbances are natural features of ecosystems that promote variability in the community and ultimately maintain diversity. Although it is recognized that global change will affect environmental disturbance regimes, our understanding of the community dynamics governing ecosystem recovery and the maintenance of functional diversity in future scenarios is very limited. Here, we use one of the few ecosystems naturally exposed to future scenarios of environmental change to examine disturbance and recovery dynamics. We examine the recovery patterns of marine species from a physical disturbance across different acidification regimes caused by volcanic CO_2 vents. Plots of shallow rocky reef were cleared of all species in areas of ambient, low, and extreme low pH that correspond to near-future and extreme scenarios for ocean acidification. Our results illustrate how acidification decreases the variability of communities, resulting in homogenization and reduced functional diversity at a landscape scale. Whereas the recovery trajectories in ambient pH were highly variable and resulted in a diverse range of assemblages, recovery was more predictable with acidification and consistently resulted in very similar algal-dominated assemblages. Furthermore, low pH zones had fewer signs of biological disturbance (primarily sea urchin grazing) and increased recovery rates of the dominant taxa (primarily fleshy algae). Together, our results highlight how environmental change can cause ecosystem simplification via environmentally mediated changes in community dynamics in the near future, with cascading impacts on functional diversity and ecosystem function.

carbonate chemistry | habitat patchiness | resilience | emergent effects | species interaction

Although there has been significant progress in understanding how environmental change can affect the abundance and distribution of individual species, considerably less is known about the effects on community dynamics and ecosystem function. Disturbance creates spatial and temporal variability in community structure across terrestrial, aquatic, and marine ecosystems (1–3), due to the removal of species from a community that allows competitively inferior species to establish and persist. This results in a patchy mosaic of assemblages, thereby maintaining diversity at the landscape scale (4). Numerous processes influence habitat patchiness, including the frequency and intensity of disturbances and the resilience of the community, which is dependent on resistance (i.e., ability of the assemblage to absorb a disturbance without changing ecosystem function) and recovery (5). Although substantial research has focused on how environmental change will influence disturbance regimes (3, 6, 7), a major question remains about how it will affect the community dynamics that govern recovery patterns and ecosystem function (2).

As environmental conditions change, there is a concern that ecosystems will become more simplified, with reduced spatial variability (8). Whereas it is readily apparent that species extinctions could contribute to an ecosystem simplification, it is less clear whether the more gradual changes in species performance could lead to the same result (9). In the ocean, the process of ocean acidification represents a pervasive environmental change that threatens to affect a wide range of species (10). The absorption of atmospheric CO_2 causes a decrease in seawater pH and carbonate ion concentrations, while increasing CO_2 and bicarbonate ion concentrations (11). Studies suggest that calcareous species that rely on carbonate ions to build their shells or skeletons of calcium carbonate could suffer reductions in calcification and ultimately abundance in an acidified ocean (10). Furthermore, studies in naturally acidified ecosystems suggest that acidification can cause an entire reorganization of marine communities (12–15), but little is known about the ecological mechanisms underlying these changes and the consequences for ecosystem function.

Similar to other environmental changes, ocean acidification has the potential to affect both the disturbance regime and the recovery of the community. Herbivory is a natural disturbance that can cause habitat patchiness (16–18) by limiting the abundance of dominant plant species and facilitating the persistence of other species that would be outcompeted and/or overgrown (18, 19). In marine ecosystems, calcareous invertebrate herbivores, including sea urchins and herbivorous snails, play fundamental roles in structuring communities by creating disturbances (20–23) and are thought to be some of the most vulnerable species to ocean acidification (10). Thus, the direct effects of ocean acidification on these grazers could have cascading impacts on disturbance regimes and diversity. Furthermore, ocean acidification may also affect recovery dynamics. Whereas acidification may slow the growth rates of some calcareous species (10), it may also increase the growth rates of noncalcareous algae due to increased concentrations of the chemical substrates used for photosynthesis (24). This could potentially alter competitive interactions between calcareous species and fleshy algae by slowing the recovery of calcareous species from disturbance (25) and promoting a shift toward noncalcified, macroalgal-dominated communities (26–29).

Recovery patterns, which are influenced by the external environment, recruitment rates, and species interactions (30, 31), can lend insight into these important community dynamics. Highly variable and idiosyncratic recovery patterns (i.e., contingent succession, *sensu* ref. 32) suggest that recovery is dependent on recruitment patterns and species interactions that vary either spatially and/or temporally (33). However, strong predictable species interactions can also cause succession to be canalized (32), in which disturbed assemblages converge on a predictable community over time (30, 31, 34). This pattern of predictable species interactions and canalized succession could be driven by harsh environmental conditions, such as ocean acidification, in which species that can tolerate or benefit from the extreme

Author contributions: K.J.K., M.C.G., and F.M. designed research; K.J.K. and M.C.G. performed research; K.J.K. analyzed data; and K.J.K. wrote the paper.

The authors declare no conflict of interest.

This article is a PNAS Direct Submission.

Freely available online through the PNAS open access option.

[1]To whom correspondence should be addressed. E-mail: kjkroeker@ucdavis.edu.

This article contains supporting information online at www.pnas.org/lookup/suppl/doi:10.1073/pnas.1216464110/-/DCSupplemental.

conditions are the only species that are able to persist through time (35, 36). Whereas contingent succession promotes a patchy mosaic landscape, canalized succession promotes a homogenous landscape.

Here, we tested how ocean acidification affects the disturbance regimes and recovery patterns of benthic rocky reef assemblages, which comprise one of the most diverse and spatially complex ecosystems of the Mediterranean (37). We monitored sea urchin populations and the recovery of permanent plots cleared of all species in three zones that vary in pH and carbonate chemistry surrounding natural volcanic CO_2 vents. These CO_2 vents, found off the coast of Italy, create gradients in pH and carbonate chemistry by releasing predominantly CO_2 with very small amounts of other gases at ambient temperatures and salinities at 2–3 m water depth on either side of a small island, characterized by shallow rocky reef communities (13). For this experiment, we delineated three pH zones (ambient, low, and extreme low pH) at two sites (north and south sides of the island) (14). The conditions in the ambient pH zones are comparable to current conditions in the surface waters in the Mediterranean Sea (Table 1). The conditions in the low pH zones are most comparable to near-future (i.e., 2100) scenarios, whereas those in the extreme low pH zones correspond to more extreme scenarios based on high CO_2 emissions or the more distant future (e.g., 2500) (38) (Table 1). The two most common sea urchins at this site, *Arbacia lixula* and *Paracentrotus lividus*, routinely graze fleshy algae (18, 23, 39).

We monitored recovery trajectories in the cleared plots for 32 mo by estimating the percent cover of nine key functional groups and bare rock (Table S1) in photos taken at 0, 1, 3, 6, 14, 20, and 32 mo after the initial clearing. Functional groups included: (*i*) biofilm and filamentous algae, (*ii*) encrusting fleshy algae, (*iii*) encrusting calcareous algae (including crustose coralline algae, CCA), (*iv*) fleshy turf algae, (*v*) calcareous turf algae, (*vi*) erect fleshy algae, (*vii*) erect calcareous algae, (*viii*) calcified filter feeders, and (*ix*) sponges. In addition, we compared the community structure in disturbed plots to photos of undisturbed reference plots taken at the time of the initial clearing to estimate recovery. Last, we quantified the abundance and size of *A. lixula* and *P. lividus* as well as their signs of grazing (i.e., sea urchin halos) (17) across pH. Our results reveal different recovery patterns among pH zones that result in less spatial and temporal variability [i.e., canalized succession; *sensu* ref. 32) in benthic communities from lower pH conditions. Furthermore, our results suggest that reduced herbivory by sea urchins in low pH and/or faster recovery rates of fleshy algae in acidified conditions could play important roles in driving these differences. Together, our results provide a unique example of how environmentally driven changes in community dynamics could result in more homogenous and predictable assemblages with cascading impacts on functional diversity and ecosystem function.

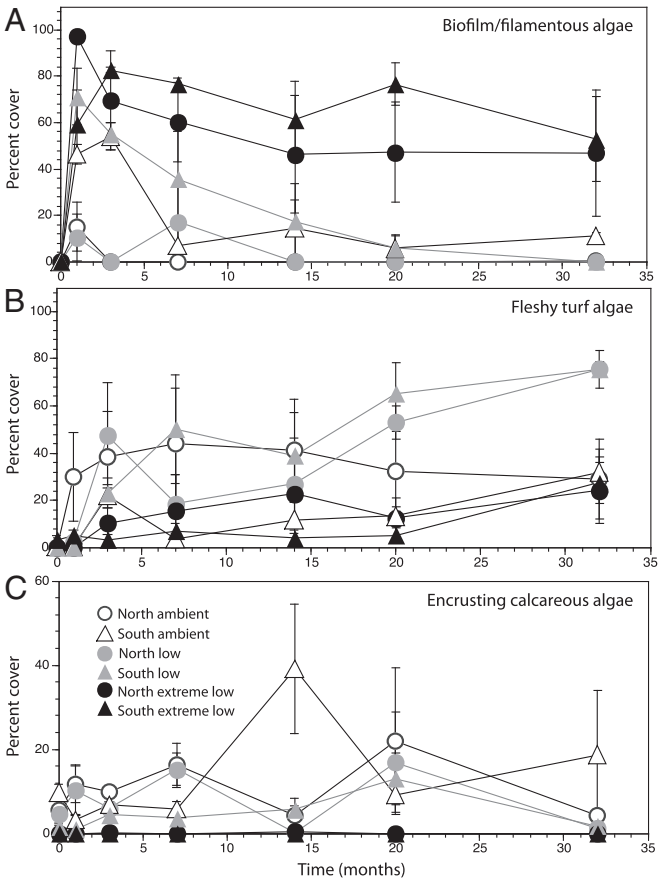

Fig. 1. Percent cover of (*A*) biofilm/filamentous algae, (*B*) fleshy turf algae, and (*C*) crustose coralline algae through time. Means ± SEM, $n = 4$.

Results

Following experimental clearings, recovery differed among pH zones. Biofilm/filamentous algae dominated the very early stages of succession in the ambient pH zones (Fig. 1*A*). Along with establishment of calcified filter feeders, CCA, erect fleshy algae, and sponges at relatively low percent cover, there was also a steady increase in the percent cover of fleshy turf algae for the first 3 mo. After 6 mo, however, the percent cover of all functional groups in the ambient pH zones showed high variability among plots (evident in the large error bars at each time point; Fig. S1), between sites (evident in the opposing fluctuations in high/low percent cover among the north and south sites in CCA; Fig. 1*C*), and among dates at both sites (evident in the sharp

Table 1. Key environmental and biogeochemical parameters in experimental pH zones in the north and south

pH zone	Temp, C	pH_T	TA	pCO_2	HCO_3^-	CO_3^{2-}	$\Omega_{calcite}$
Ambient, N	23.4 ± 0.7	8.0 ± 0.1	2,563 ± 3	568 ± 100	2,059 ± 54	202 ± 22	4.8 ± 0.5
Ambient, S	19.6 ± 1.5	8.1 ± 0.1	2,563 ± 2	440 ± 192	2,016 ± 71	219 ± 29	5.1 ± 0.7
Low, N	23.8 ± 0.7	7.8 ± 0.2	2,560 ± 7	1,075 ± 942	2,180 ± 115	150 ± 47	3.5 ± 1.1
Low, S	17.5 ± 2.8	7.8 ± 0.3	2,560 ± 7	1,581 ± 2,711	2,232 ± 136	128 ± 56	3.0 ± 1.3
Extreme low, N	23.4 ± 0.7	7.2 ± 0.4	2,559 ± 13	6,590 ± 21,352	2,428 ± 85	54 ± 35	1.3 ± 0.8
Extreme low, S	17.5 ± 2.8	6.6 ± 0.5	2,563 ± 13	23,989 ± 16,638	2,508 ± 100	21 ± 41	0.5 ± 0.9

The pH and temperature estimates are based on hourly measurements from in situ pH meters taken during separate deployments for N and S sites [N = 604 (north) –3162 (south)]. Total alkalinity (TA) and salinity estimates (mean 38 ppm) are from discrete water samples taken throughout sensor deployments (n = 3–10), and all other carbonate parameters are estimated by assuming constant TA and salinity and applying the mean TA and salinity values to pH and temperature values measured by in situ sensors. Differences in temperature between sites are due to deployment times: early summer (north) and early fall (south). Values are means ± SD. TA, HCO_3^-, CO_3^{2-} are reported in $\mu mol \cdot kg^{-1}$.

peaks of CCA and calcified filter feeder percent cover through time; Fig. 1*C* and Fig. S1).

In the low pH zones, biofilm/filamentous algae, calcified filter feeders, CCA, and fleshy turf algae all became established in the early stages of succession (Fig. S1). Whereas the percent cover of biofilm/filamentous algae decreased steadily until it was nearly absent by 32 mo (Fig. 1*A*), turf algae increased steadily throughout the time series (Fig. 1*B*) with an exception at the northern site at 6 mo when there was a reduction in cover. This occurred during a period of high percent cover of erect fleshy algae typical during this part of the year (Fig. S1). The percent cover of calcified filter feeders and CCA remained around 1%, with minor temporal variability throughout the rest of the time series (Fig. S1).

In the extreme low pH, the percent cover of biofilm/filamentous algae increased sharply in the first 1–3 mo of succession and remained high throughout recovery (Fig. 1*A*). All growth forms of fleshy algae (encrusting, turf, and erect) showed increasing trends for the first 3 mo, then moderate variability for the rest of the time series (Fig. S1). Calcareous species were very rarely found in the extreme low pH zones.

These recovery patterns resulted in significantly different communities among pH zones after 32 mo (Fig. 2, Table 2, and Table S2). The differences were primarily due to a higher abundance of calcareous algae in ambient pH versus a higher abundance of fleshy algae in the low pH zones. In contrast, biofilm/filamentous algae and erect fleshy algae dominated the extreme low pH zones. In addition, there is greater variability in the communities in the ambient and extreme low pH zones than those in the low pH (Fig. 3*A* and Table S2). These patterns reflect those in background communities in each pH zone (Figs. S2 and S3).

We calculated the Spearman correlations between pairs of recovery trajectories to compare the patterns of change irrespective of differences due to community composition (40). Using this "second-stage analysis" it is apparent that the patterns of community change (i.e., the similarity in communities between successive time steps) differed among pH zones regardless of which functional groups constituted the community (Fig. 3*B*, Table 2, and Table S3). The recovery in ambient pH was much more variable than in the extreme low and low pH zones (Fig. 3*B* and Table 2), which both showed consistent changes through time.

The similarity between the community structure of disturbed plots with undisturbed, reference plots from the beginning of the experiment further highlights differences in the recovery dynamics among pH zones. There was a sharp increase in the similarity between disturbed and reference plots in the extreme low pH in the first 3 mo postclearing (Fig. 4*A*), indicating a rapid recovery of plots in extreme low pH. In contrast, the similarity between disturbed and reference plots increased more gradually through time in both the low and ambient pH, with more marked temporal variability (Fig. 4*A*).

Table 2. Summary statistics table for tests of differences among pH zones (neither *site* × pH or site were significant for any test)

Analysis	df	*F*	*P*	Pairwise comparisons
Community structure (CS)	2.23	8.0	<0.001	A ≠ L ≠ XL
Variability in CS	2.21	8.9	0.004	L ≠ A or XL; A = XL
Recovery trajectories	2.23	2.6	0.02	XL ≠ A or L; A = L
Variability in recovery trajectories	2.21	14.9	<0.001	A ≠ L or XL; L = XL
Amount of change through time	2.18	5.4	0.01	XL ≠ A or L; A = L

To examine why recovery rates differed among pH zones, we quantified the relative amounts of change in the communities through time. By plotting the disturbed communities through time in a nonmetric multidimensional scaling (nMDS) ordination based on Bray–Curtis (BC) similarities, we were able to calculate the distance traveled in 2D nMDS space of each plot over 32 mo (41). Because distance represents differences between communities in an nMDS ordination, longer distances traveled represent greater changes in the assemblage over time. This analysis revealed the least amount of community change in extreme low pH (i.e., the shortest distance traveled; Fig. 4*B*, Table 2, and Table S4).

We did not detect differences in the mean abundance or size of *A. lixula* or *P. lividus* between the ambient and low pH zones (Fig. S4 and Table S5). However, the number of sea urchin halos in the low pH zones was significantly less than that in the ambient pH zones [Fig. 5; repeated measures (RM)-ANOVA pH $F_{1,2} = 19.30$, $P = 0.05$] and was not significantly different between sampling dates [RM-ANOVA within subjects test for date $F_{2,4} = 3.87$, Greenhouse–Geisser (GG) adjusted $P = 0.17$, and date × pH $F_{2,4} = 2.28$, GG adjusted $P = 0.27$]. No sea urchins and no grazing halos were observed in the extreme low pH zones.

Discussion

Our results reveal how altered community dynamics in conditions representing future environmental scenarios reduce the natural variability in community structure, resulting in more homogeneous and simplified communities. The recovery patterns of benthic assemblages associated with CO_2 vents highlight how the highly variable, contingent recovery patterns that characterize current conditions are more canalized with acidification,

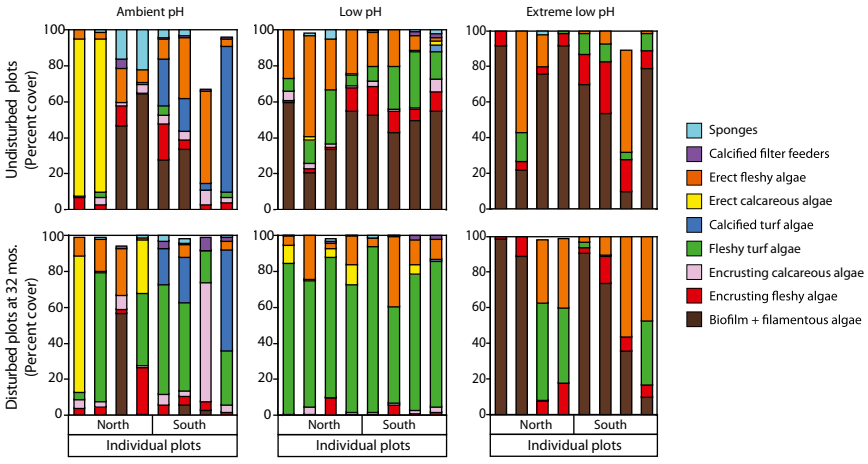

Fig. 2. Community structure in undisturbed, reference plots vs. experimental plots after 32 mo of recovery among pH zones. Each bar represents a single plot.

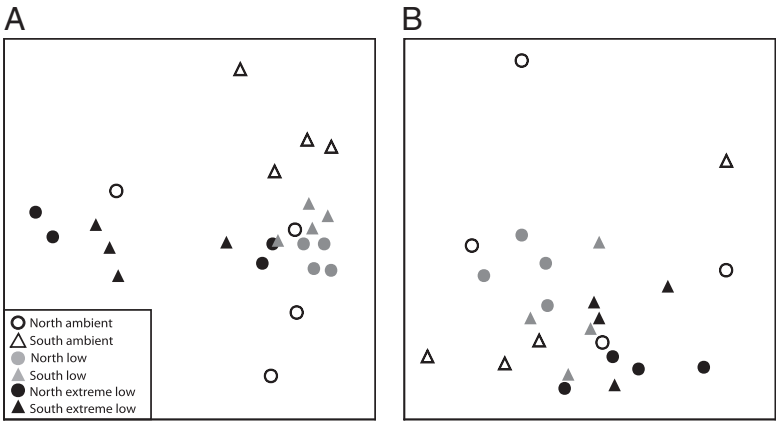

Fig. 3. nMDS plots highlighting variation in (*A*) community structure and (*B*) patterns of recovery. Distance between points represents differences in (*A*) the assemblages at 32 mo postdisturbance and (*B*) the patterns of change through time for each plot for the entire recovery period. Fig. 3*B* represents differences in the correlation structure between time points for a single plot that are independent of the identity of taxa (i.e., whether recovery itself was similar or variable among plots). Means ± SEM, $n = 4$.

resulting in homogenous assemblages. Thus, our results reveal how an environmentally mediated reorganization of a community that favors species with high physiological tolerance and rapid growth can result in decreased patchiness and lower functional diversity.

The stochastic and variable succession in ambient pH suggests that the recovery patterns are contingent on species interactions (32). Indeed, the sharp peaks in percent cover of calcified filter feeders and CCA and the corresponding reductions in fleshy algae (Fig. 1 and Fig. S1) were driven by plots near or within sea urchin halos (Fig. S5). This suggests sea urchins influenced the variability in succession and community structure in ambient pH plots by grazing fleshy algae and exposing CCA and new substrate for competitively inferior species (23). Therefore, the wide range of assemblage types in ambient pH was potentially influenced by periodic disturbances (grazing) that resulted in plots being at several different stages of succession.

In contrast, the homogeneity of the low pH assemblages at 32 mo (Fig. 3*A*) and the similarity of recovery trajectories in these conditions (Fig. 3*B*) reveal more restricted succession in the low pH zones. Our results illustrate how assemblages in acidified conditions representative of near future conditions follow a repeatable pattern of recovery that converges on an overall simplified, turf-dominated community (Fig. S2). Coupled with our observations regarding the reduced number of sea urchin halos in low pH, these patterns suggest there is a potential for reduced biotic disturbance and habitat patchiness with acidification.

The greater number of sea urchin halos in the ambient compared with low pH zones also suggests that sea urchins may play a different functional role in acidified conditions. Because sea urchins of similar sizes were regularly present in the low pH zones and consistently found in the same locations over the 3-y period (suggesting that the sea urchins in low pH were semipermanent features of this zone), the most likely mechanisms for the reduction in sea urchin halos include reduced grazing rates due to physiological and behavioral impacts on sea urchins (10) and/or increased growth rates of algae in response to the increased carbon supply (24). In addition, changes in the nutrient quality or chemistry of the algae could contribute to altered grazing rates or strategies (selective grazing) of sea urchins in low pH. However, an important distinction between the vent ecosystem and future scenarios of ocean acidification is that sea urchin larvae can originate from nonacidified source regions, which would not be the case in an acidified ocean. Thus, if there are bottlenecks in species tolerance to acidification caused by reproduction or larval survival, these effects could be underestimated at the vent site.

There were essentially two assemblage types in extreme low pH: either biofilm/filamentous algae or erect fleshy algae (Fig. 2). Although this represents a form of habitat patchiness, it differs from the patchy mosaic in ambient pH because it consists of only two very simple and depauperate assemblages. This increased dominance of biofilm/filamentous algae, whose production may be enhanced by acidification (42), is likely to have repercussions for higher trophic levels because it lacks much of the 3D structure that serves as habitat for other organisms. Furthermore, it remains to be tested whether the absence of sea urchins in extreme low pH is a result of a physiological intolerance or in response to the changing algal community. Whereas laboratory studies suggest *P. lividus* is resistant to low pH (43), studies of other echinoderms have reported sharp reductions in survival below pH 7.0 (44).

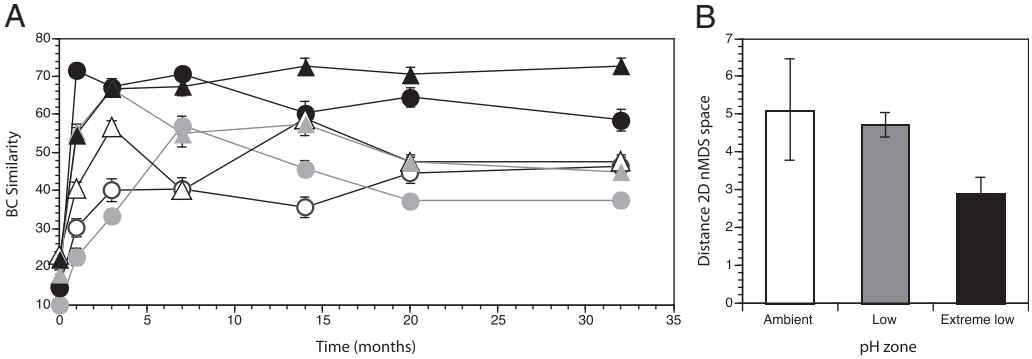

Fig. 4. Recovery dynamics of disturbed plots across pH zones. (*A*) Mean similarity among undisturbed reference plots at the beginning of the experiment with disturbed plots through time (Mean ± SEM, $n = 16$). (*B*) Mean distance traveled by each plot in 2D nMDS space from clearing to 32 mo (mean ± SEM, $n = 8$). Circles, north; triangles, south; white, ambient pH; gray, low pH; black, extreme low pH.

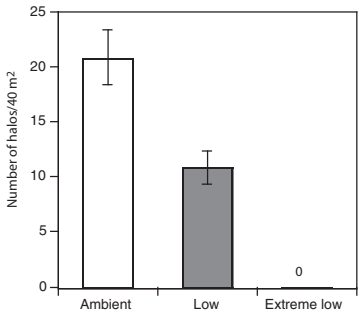

Fig. 5. Total number of sea urchin halos in pH zones. Means ± SEM, $n = 3$, based on repeated measurements in each site x pH zone in June 2009, May 2010, and October 2010.

Whereas previous research has suggested that assemblages with high diversity will be more resilient and recover more quickly than less diverse communities (45), our analyses highlight the most rapid recovery in the extreme low pH assemblages typified by low functional diversity (Fig. 4*A*). Whereas this is likely because succession to this simplified state is inherently shorter (Fig. 4*B*), our results illustrate how highly impacted assemblages can have very high resilience once in an oversimplified or degraded state. However, acidification is only one aspect of environmental change, and the cumulative impacts of additional press disturbances that affect ecosystem resilience (e.g., warming or overfishing) and pulse disturbances (e.g., storms and pollution events) that will likely co-occur with acidification require further attention (1, 46, 47).

In conclusion, our results provide a unique example of how environmentally mediated changes in complex community dynamics could cause ecosystem simplification under projected future environmental conditions. In particular, the patterns in community recovery and grazing in the naturally acidified ecosystem revealed here suggest that one of the most pervasive environmental changes in the ocean could cause a decrease in the patchiness and functional diversity of benthic marine communities. Furthermore, our results suggest that ocean acidification could cause a change in the functional role of calcareous grazers. Changes in the role of large calcareous grazers, such as sea urchins and herbivorous snails that are known to influence community structure in many different marine ecosystems (18, 20–23), could have widespread consequences for many ocean ecosystems (17, 18).

Methods

Field Site. For this experiment, we delineated three pH zones (ambient, low, extreme low pH) at two sites (north and south) that corresponded with the zones used in previous studies (14). Each zone is ∼30 m long and separated from the other pH zones by 20 m (27). Carbonate parameters were estimated from pH and temperature measurements taken every hour with in situ sensors (48) that were deployed during the time of this experiment. In the south, separate month-long deployments were made in fall 2009 as well as winter, spring, and fall 2010, whereas deployments were limited to fall 2010 in the north (Table S6) (14). We collected discrete water samples during the sensor deployment following standard operating procedures, and measured dissolved inorganic carbon (UIC automated 5011 coulometer) and total alkalinity (open cell potentiometric titrator), and salinity (Guildline Autosal salinometer) in each sample. We then calculated the pH in the discrete water samples using Seacarb v. 2.3.2 (49), by applying the temperature measured at the time of the collection, and used this calculated pH value to calibrate the initial readings from the sensors. We then estimated the biogeochemical parameters by assuming a constant total alkalinity and salinity and applying the pH and temperature values measured by the in situ sensors through time (see ref. 14 for more in-depth discussion of methods). Whereas mean pH was predictably lower in winter and spring (during the coldest temperatures), the differences among and the variability within these zones were consistent across seasons (Table S6) (14).

There is high temporal variability in carbonate chemistry and pH near the vents, with highest variability in the extreme low pH zones (14). Monitoring in other nearshore environments suggest that high variability in carbonate chemistry and pH is a natural feature in other ecosystems as well (48). Whereas it would be ideal to tease apart the effects of mean changes in the carbonate chemistry from the variability in carbonate chemistry, this is not possible at this site because reductions in mean pH covary with increased pH variability. Results and ecological patterns should be considered in terms of responses to carbonate chemistry/pH regimes (which include variability) rather than to mean estimates of biogeochemical parameters.

Experimental Manipulations. Plots (20 × 20 cm) were cleaned with wire brushes and marked at the corners with epoxy in March 2009 ($n = 4$ for each pH zone). Brushing removed all sessile macroinvertebrates and algae. Plots were chosen haphazardly in each zone and were separated by at least 3 m. Plots were chosen to have minimal rugosity and were approximately vertical in orientation (95–115° from the bottom substrate) at 1–1.5 m depth. By nature of the site, plots in the north were north–northwest facing, whereas those in the south were south–southeast facing (14). Although this is likely to result in differences in exposure between sites, significant pH effects were detected above and beyond any site variability (Tables S2–S4), suggesting the pH effects are robust to the inherent differences between sites.

Plots were photographed in situ at 0, 1, 3, 6, 14, 20, and 32 mo after the initial clearing. In addition, we took photos of undisturbed plots directly adjacent to clearings (within 10 cm of disturbed plots) in March 2009 ($t = 0$). Taxa were then identified to the lowest taxonomic resolution possible in photos and then grouped into the nine functional groups, plus a category for bare rock (Table S1). Turf and erect algal designations were based on sizes, with turf being less than ∼10 cm tall. Calcareous turf algae were kept separate from erect calcareous algae because of the potential for non-calcareous turfs to be mixed in with the dominant calcareous turfs. Percent cover was estimated with photo analysis software (Vidana v1.1). Because percent cover was estimated from photos, we did not estimate taxa underneath the layers visible in the photos. Whereas this probably reduced our detection of cryptic species, photo quadrats allowed us to nondestructively sample the same plots through time and provide reliable estimates of percent cover of broad functional groups (50).

Sea Urchin Estimates. We counted and measured all *A. lixula* and *P. lividus* with calipers along 20 × 2 m transects that ran through the plots at 1.5-m depth. These transects were resampled in June 2009, May 2010, and October 2009 and 2010. In addition, we counted and measured the vertical and horizontal lengths of all sea urchin grazing halos along the transects. We defined sea urchin halos as areas of substrate devoid of fleshy algae, within 50-cm distance from a sea urchin. We then estimated the area of each halo by assuming the shape of the halos were ellipses and using standard area formulas.

Statistical Analyses. Community structure was estimated by calculating a BC similarity matrix of the square-root transformed percent cover of functional groups in each plot. The BC similarity is calculated as the sum of the differences in percent cover of each functional group between plots divided by the sum of the total percent cover of the functional groups in both plots. The square-root transformation emphasizes the importance of rarer functional groups (e.g., CCA, which is rarely above 5% cover), and the inclusion of bare rock as a category allowed us to define denuded assemblages as completely similar. Variation in the community structure was compared using permutational multivariate analysis of variance (PERMANOVA) with site and pH as fixed factors and type III sums of squares. The permutation routine is a randomization procedure where the factor labels (site and pH) are randomly shuffled among the samples 9,999 times. Each time a new F statistic is calculated, and the probability is calculated as the proportion of the F values that are greater or equal to the observed F statistic. In addition, we performed the same analyses on raw data to understand the role of data transformation on our results. The general results did not differ between the raw and transformed data, and we report the transformed analyses in the text.

Variation in the recovery trajectories (e.g., the pattern of change through time) was compared with a second-stage analysis, which is performed by calculating Spearman correlations between BC similarity matrices of individual plots through time (39). Significant differences among pH zones in this analysis indicate there are differences in similarities between successive time steps for a particular plot that are independent of the identities of functional groups.

We also compared dispersion of the recovery trajectories and resulting communities with permutational analysis of multivariate dispersions (PERMDISP), which is essentially a nonparametric, multivariate analog of Levene's test for

homogeneity of variance. This was done by calculating the dissimilarities among trajectories or plots and running a principal coordinates analysis (PCoA) on the dissimilarity matrix. We then calculated the centroids for each pH zone based on the PCoA axes and then calculated the Euclidean distance between each plot and the centroid of its pH group. These distances are then treated as univariate variables for statistical tests.

Recovery was estimated by plotting the mean similarities between all plots in each site × pH zone with reference undisturbed plots from the same site × pH zone from March 2009 (Fig. 4). We also created an nMDS ordination of each of the plots through time. We then calculated the distance traveled in 2D nMDS space of each plot between subsequent time points (41). These distances were summed to estimate the mean distance traveled in nMDS space over 32 mo of recovery, which could be used as an univariate estimate of the amount of change through time.

Variation in the abundance and size of sea urchins (both *A. lixula* and *P. lividus* separately) as well as the number and total area of sea urchin halos was tested with ANOVA with repeated measures, with site and pH zone as fixed factors, excluding extreme low pH from the analyses. GG-corrected *P* values were used for repeated measures. For all sea urchin analyses, the site factor was highly nonsignificant ($P = 0.31–0.98$) and was thus removed from the analyses to increase our power to detect differences between pH zones. The significance of the *P* value did not change in the tests of abundance or size for either sea urchin species with the removal of the site factor, but did change in the analyses of halos. Univariate repeated measures ANOVA were performed in Systat 11.

With the exception of RM-ANOVA, differences among univariate variables were tested with permutation-based ANOVA due to heterogeneity of variance. *P* values were generated by 9,999 permutations of the raw data (i.e., samples were randomly reassigned to the factors to create an *F* distribution that the observed *F* statistic is tested against). All permutation-based analyses were performed with PRIMER v6.

ACKNOWLEDGMENTS. We thank R. L. Kordas for helpful comments on an earlier version of this manuscript; A. J. Haupt, B. Iacono, Capt. V. Rando, L. Porzio, and M. C. Buia for their fieldwork assistance; as well as the staff from the Ischia benthic ecology team of the Stazione Zoologica Anton Dohrn (SZN). This research was supported by a National Science Foundation Graduate Research Fellowship (to K.J.K.), a Stanford University Chambers Fellowship (to F.M.), a Pew Fellowship in Marine Conservation (to F.M.), and the SZN.

1. Sousa WP (1979) Disturbance in marine intertidal boulder fields: The nonequilibrium maintenance of species diversity. *Ecology* 60:1225–1239.
2. Turner MG (2010) Disturbance and landscape dynamics in a changing world. *Ecology* 91(10):2833–2849.
3. Whited DC, et al. (2007) Climate, hydrologic disturbance, and succession: drivers of floodplain pattern. *Ecology* 88(4):940–953.
4. Levin SA, Paine RT (1974) Disturbance, patch formation, and community structure. *Proc Natl Acad Sci USA* 71(7):2744–2747.
5. Holling CS (1973) Resilience and stability of ecological systems. *Annu Rev Ecol Evol Syst* 4:1–23.
6. Clark JS (1988) Effect of climate change on fire regimes in northwestern Minnesota. *Nature* 334:233–235.
7. Littell JS, McKenzie D, Peterson DL, Westerling AL (2009) Climate and wildfire area burned in western U.S. ecoprovinces, 1916-2003. *Ecol Appl* 19(4):1003–1021.
8. Jackson JBC (2008) Ecological extinctions and evolution in the brave new ocean. *Proc Natl Acad Sci USA* 105:11458–11465.
9. Harley CDG (2011) Climate change, keystone predation, and biodiversity loss. *Science* 334(6059):1124–1127.
10. Kroeker KJ, Kordas RL, Crim RN, Singh GG (2010) Meta-analysis reveals negative yet variable effects of ocean acidification on marine organisms. *Ecol Lett* 13(11): 1419–1434.
11. Feely RA, Doney SC, Cooley SR (2009) Present conditions and future changes in a high-CO_2 world. *Oceanogr.* 22:36–47.
12. Fabricius KE, et al. (2011) Losers and winners in coral reefs acclimatized to elevated carbon dioxide concentrations. *Nature Climate Change* 1:1–5.
13. Hall-Spencer JM, et al. (2008) Volcanic carbon dioxide vents show ecosystem effects of ocean acidification. *Nature* 454(7200):96–99.
14. Kroeker KJ, Micheli F, Gambi MC, Martz TR (2011) Divergent ecosystem responses within a benthic marine community to ocean acidification. *Proc Natl Acad Sci USA* 108(35):14515–14520.
15. Porzio L, Buia MC, Hall-Spencer JM (2011) Effects of ocean acidification on macroalgal communities. *JEMBE* 400:278–287.
16. Huntly N (1991) Herbivores and the dynamics of communities and ecosystems. *Annu Rev Ecol Syst* 22:477–503.
17. Levings SC, Garrity SD (1983) Diel and tidal movement of two co-occurring Neritid snails: Differences in grazing patterns on a tropical rocky shore. *JEMBE* 67:261–278.
18. Bulleri F, Bertocci I, Micheli F (2002) Interplay of encrusting coralline algae and sea urchins in maintaining alternative habitats. *Mar Ecol Prog Ser* 243:101–109.
19. Hughes TP, Connell JH (1999) Multiple stressors on coral reefs: A long-term perspective. *Limnol Oceanogr* 44:932–940.
20. Lubchenco J (1978) Plant species diversity in a marine intertidal community: Importance of herbivore food preference and algal competitive abilities. *Am Nat* 112:23–39.
21. Bertness MD (1984) Habitat and community modification by an introduced herbivorous snail. *Ecology* 65:370–381.
22. Carpenter RC (1986) Partitioning herbivory and its effects on coral reef algal communities. *Ecol Monogr* 56:345–363.
23. Bulleri F, Benedetti-Cecchi L, Cinelli F (1999) Grazing by the sea urchins *Arbacia lixula* L. and *Paracentrotus lividus* Lam. in the Northwest Mediterranean. *JEMBE* 241:81–95.
24. Koch M, Bowes G, Ross C, Zhang X-H (2012) Marine macro-autotrophs and climate change. *Glob Change Biol* 19(1):103–132, 10.1111/j.1365-2486.2012.02791.x.
25. Anthony KRN, et al. (2011) Ocean acidification and warming will lower coral reef resilience. *Glob Change Biol* 17:1798–1808.
26. Russell BD, Thompson J-AI, Falkenberg LJ, Connell SD (2009) Synergistic effects of climate change and local stressors: CO_2 and nutrient-driven change in subtidal rocky habitats. *Glob Change Biol* 15:2153–2162.
27. Diaz-Pulido G, Gouezo M, Tilbrook B, Dove S, Anthony KRN (2011) High CO_2 enhances the competitive strength of seaweeds over corals. *Ecol Lett* 14(2):156–162.
28. Kroeker KJ, Micheli F, Gambi MC (2013) Ocean acidification causes ecosystem shifts via altered competitive interactions. *Nature Climate Change* 3:156–159.
29. Johnson VR, Russell BD, Fabricius KE, Brownlee C, Hall-Spencer J (2012) Temperate and tropical brown macroalgae thrive, despite decalcification, along natural CO_2 gradients. *Glob Change Biol* 18:2792–2803.
30. Connell JH, Slatyer RO (1977) Mechanisms of succession in natural communities and their role in community stability and organization. *Am Nat* 111:1119–1144.
31. Farrell TM (1991) Models and mechanisms of succession: An example from a rocky intertidal community. *Ecol Monogr* 61:95–113.
32. Berlow EL (1997) From canalization to contingency: Historical effects in a successional rocky intertidal community. *Ecol Monogr* 67:435–460.
33. Sutherland JP, Karlson RH (1977) Development and stability of the fouling community at Beaufort, North Carolina. *Ecol Monogr* 47:425–446.
34. Lubchenco J (1983) *Littorina* and *Fucus*: Effects of herbivores, substratum heterogeneity, and plant escapes during succession. *Ecology* 64:1116–1123.
35. Shank TM, et al. (1998) Temporal and spatial patterns of biological community development at nascent deep-sea hydrothermal vents. *Deep-Sea Res* 45:465–515.
36. Mullineaux LS, Peterson CH, Micheli F, Mills SW (2003) Successional mechanism varies along a gradient in hydrothermal fluid flux at deep-sea vents. *Ecol Monogr* 73: 523–542.
37. Fraschetti S, Terlizzi A, Benedetti-Cecchi L (2005) Patterns of distribution of marine assemblages from rocky shores: Evidence of relevant scales of variation. *Mar Ecol Prog Ser* 296:13–29.
38. Caldeira K, Wickett ME (2003) Oceanography: Anthropogenic carbon and ocean pH. *Nature* 425(6956):365.
39. Benedetti-Cecchi L, Bulleri F, Cinelli F (1998) Density dependent foraging of sea urchins in shallow subtidal reefs on the west coast of Italy (western Mediterranean). *Mar Ecol Prog Ser* 163:203–211.
40. Clarke K, Somerfield P, Airoldi L, Warwick R (2006) Exploring interactions by second-stage community analyses. *JEMBE* 338:179–192.
41. Vinebrooke RD, Graham MD, Findlay DL, Turner MA (2003) Resilience of epilithic algal assemblages in atmospherically and experimentally acidified boreal lakes. *Ambio* 32(3):196–202.
42. Lidbury I, Johnson VR, Hall-Spencer JM, Munn CB, Cunliffe M (2012) Community-level response of coastal microbial biofilms to ocean acidification in a natural carbon dioxide vent ecosystem. *Mar Pollut Bull* 64(5):1063–1066.
43. Martin S, et al. (2011) Early development and molecular plasticity in the Mediterranean sea urchin *Paracentrotus lividus* exposed to CO_2-driven acidification. *JEB* 214: 1357–1368.
44. Clark D, Lamare M, Barker M (2009) Response of sea urchin pluteus larvae (Echinodermata: Echinoidea) to reduced seawater pH: A comparison among tropical, temperate and polar species. *Mar Biol* 156:1125–1137.
45. Yachi S, Loreau M (1999) Biodiversity and ecosystem productivity in a fluctuating environment: The insurance hypothesis. *Proc Natl Acad Sci USA* 96(4):1463–1468.
46. Airoldi L (2000) Responses of algae with different life histories to temporal and spatial variability of disturbance in subtidal reefs. *Mar Ecol Prog Ser* 195:81–92.
47. Bulleri F, Benedetti-Cecchi L (2006) Mechanisms of recovery and resilience of different components of mosaics of habitats on shallow rocky reefs. *Oecologia* 149(3):482–492.
48. Hofmann GE, et al. (2011) High-frequency dynamics of ocean pH: A multi-ecosystem comparison. *PLoS ONE* 6(12):e28983.
49. Lavigne H, Gattuso JP (2010) Seacarb: Seawater carbonate chemistry with R. R package version 235.
50. Meese RJ, Tomich A (1992) Dots on the rocks: A comparison of percent cover estimation methods. *JEMBE* 165:59–73.